

LA-UR-

09-07753

Approved for public release;  
distribution is unlimited.

*Title:* SHOCK INITIATION STUDIES ON HIGH  
CONCENTRATION HYDROGEN PEROXIDE

*Author(s):* STEPHEN A. SHEFFIELD, DANA M. DATTELBAUM,  
DAVID B. STAHL, L. LEE GIBSON, AND BRIAN D.  
BARTRAM  
GROUP DE-9, LOS ALAMOS NATIONAL LAB.

*Intended for:* 2009 JOINT ARMY-NAVY-NASA-AIR FORCE (JANNAF)  
MEEETING  
LA JOLLA, CA  
DECEMBER 7-11, 2009



Los Alamos National Laboratory, an affirmative action/equal opportunity employer, is operated by the Los Alamos National Security, LLC for the National Nuclear Security Administration of the U.S. Department of Energy under contract DE-AC52-06NA25396. By acceptance of this article, the publisher recognizes that the U.S. Government retains a nonexclusive, royalty-free license to publish or reproduce the published form of this contribution, or to allow others to do so, for U.S. Government purposes. Los Alamos National Laboratory requests that the publisher identify this article as work performed under the auspices of the U.S. Department of Energy. Los Alamos National Laboratory strongly supports academic freedom and a researcher's right to publish; as an institution, however, the Laboratory does not endorse the viewpoint of a publication or guarantee its technical correctness.

## SHOCK INITIATION STUDIES ON HIGH CONCENTRATION HYDROGEN PEROXIDE

S. A. Sheffield, D. M. Dattelbaum, D. B. Stahl, L. L. Gibson, and B. D. Bartram  
Los Alamos National Laboratory/Shock and Detonation Physics Group  
Los Alamos, NM 87144

### ABSTRACT

Concentrated hydrogen peroxide ( $H_2O_2$ ) has been known to detonate for many years. However, because of its reactivity and the difficulty in handling and confining it, along with the large critical diameter, few studies providing basic information about the initiation and detonation properties have been published. We are conducting a study to understand and quantify the initiation and detonation properties of highly concentrated  $H_2O_2$  using a gas-driven two-stage gun to produce well defined shock inputs. Multiple magnetic gauges are used to make in-situ measurements of the growth of reaction and subsequent detonation in the liquid. These experiments are designed to be one-dimensional to eliminate any difficulties that might be encountered with large critical diameters. Because of the concern of the reactivity of the  $H_2O_2$  with the confining materials, a remote loading system has been developed. The gun is pressurized, then the cell is filled and the experiment shot within less than three minutes. TV cameras are attached to the target so the cell filling can be monitored. Several experiments have been completed on ~98 wt %  $H_2O_2/H_2O$  mixtures; initiation has been observed in some experiments that shows homogeneous shock initiation behavior. The initial shock pressurizes and heats the mixture. After an induction time, a thermal explosion type reaction produces an evolving reactive wave that strengthens and eventually overdrives the first wave producing a detonation. From these measurements, we have determined unreacted Hugoniot information, times (distances) to detonation (Pop-plot points) that indicate low sensitivity, and detonation velocities of high concentration  $H_2O_2/H_2O$  solutions that agree with earlier estimates.

### INTRODUCTION

Hydrogen peroxide/water ( $H_2O_2/H_2O$ ) mixtures are known to be highly reactive, detonable solutions.<sup>1-3</sup> Interrogation of their behaviors under shock compression is of interest for several reasons: 1) they are chemically simple, i.e. they are composed of only hydrogen and oxygen making their detonation products uncomplicated, and spectroscopic interrogations of their shock-induced reactions a possibility; 2) very little is known about the detonation and initiation properties of the mixtures at high peroxide concentrations; 3) these materials are used in rocket propulsion applications, 4) large quantities are used (and transported) for commercial purposes, and 5) highly concentrated hydrogen peroxide solutions and their mixtures with other organic compounds yield detonable mixtures.

Here, we describe the results of *preliminary* shock compression and initiation experiments on highly concentrated hydrogen peroxide/water solutions. Unreacted Hugoniot data, derived from gas gun-driven plate impact experiments on >95 %  $H_2O_2/H_2O$  solutions, are presented and compared with predictions based on a relationship known as the Universal Liquid Hugoniot (ULH).<sup>4</sup> Evidence of initiation in some of the plate impact experiments is discussed in the context of explosive initiation mechanisms and earlier work on nitromethane (NM) and NM:diethylene triamine (DETA) related relevant liquid explosives. Comparisons between the detonation properties measured here, and predictions made in Ref. 1 are also presented.

While hydrogen peroxide/water solutions are known to be detonable mixtures, the details about which concentrations support self-sustained detonations remain unclear. A complicating feature in attempting to discern the limits of initiation and detonability of these solutions (or any explosive for that matter) is the wide variation in experimental configurations, leading to difficulties in drawing generalized conclusions. Detonation, in most situations, is a multi-dimensional

process with characteristics (velocity, critical diameter, front curvature) that are strongly dependent on geometry and confinement, initial temperature, stimuli or initiation source, and material features (microstructure, presence or absence of bubbles, impurities, porosity, etc.). The goal of this work is to provide equation of state data and shock initiation data on a range of concentrations of  $\text{H}_2\text{O}_2/\text{H}_2\text{O}$  solutions in one-dimensional shock experiments. Here, we present the results of our preliminary efforts in obtaining shock initiation data on ~98 and 95 wt%  $\text{H}_2\text{O}_2/\text{H}_2\text{O}$  solutions.

Almost a decade ago, an extensive literature search was performed seeking detonation information on high concentration  $\text{H}_2\text{O}_2$  solutions, with very little success. Some information was found, but almost none of it provided quantitative evaluation of initiation and detonation properties. Extensive compilations of physical and chemical data on  $\text{H}_2\text{O}_2$  are available in Ref. 2. There have been studies of the detonation of  $\text{H}_2\text{O}_2/\text{H}_2\text{O}$  mixtures in the *vapor phase*; see, e.g., Ref. 5 and references therein. In contrast to this, very little quantitative published work on the detonation properties of liquid-phase  $\text{H}_2\text{O}_2/\text{H}_2\text{O}$  mixtures exists. In Ref. 6, evidence is presented that liquid 86/14 wt %  $\text{H}_2\text{O}_2/\text{H}_2\text{O}$  mixture is detonable. A rough detonation speed of ca. 6000 m/s (measured using a streak camera) is inferred from the data for this mixture. The initial shot temperature and the tube diameter are both unspecified, but the confining tube material is specified as steel. Much of the information in this reference pertains to  $\text{H}_2\text{O}_2/\text{H}_2\text{O}/\text{alcohol}$  mixtures which is not relevant to this paper.

Also, in Ref. 7, results on the critical diameters of liquid 86.0/14.0 and 90.7/9.3 wt (?) %  $\text{H}_2\text{O}_2/\text{H}_2\text{O}$  mixtures confined in 61STS Al tubes with inner diameters of 26.7, 31.8, and 40.9 mm and initial temperatures between 25 and 70 °C and are given. The authors conclude that, for the 86% material, the critical diameter is ca. 40.6 mm at 50 °C and 35.6 mm at 70 °C and, for the 90.7% material, the critical diameter decreased from 40.6 mm at 25 °C to 20.3 mm at 70 °C. Rough detonation speed measurements gave speeds in the range 5500-6000 m/s. However, there is some concern about these experiments because of the aluminum confinement and the fact that the shock speed in the confiner may exceed the detonation velocity. This would lead to erroneous measurements.

Early work on the safety characteristics, detonation properties, and combustion and explosion limits of liquid and vapor phase  $\text{H}_2\text{O}_2$  was performed during World War II by the Germans. A summary of this work is presented in a Shell Chemical Company report,<sup>2</sup> which had the purpose of establishing safety guidelines for large production quantities of  $\text{H}_2\text{O}_2$ . In the early work, the Germans found that stoichiometric mixtures of 85.7 wt(?)%  $\text{H}_2\text{O}_2$  and organic compounds (methanol, ethanol, glycerol) exhibited detonation velocities in the range of 6000-7000 m/s. These solutions were initiated by blasting caps or PETN. Further, their experiments gave insight into diameter effect behaviors of the mixtures. Figure 1 shows the measured detonation velocities as a function of  $1/R$  ( $R$  = charge radius, cm). Inspection of the figure reveals that; 1) there is a lot of scatter in the data, likely due to the variation in the materials tested (bubbles, how well mixed, time between mixing and firing, etc.), and 2) the measured detonation velocities were higher for the glycerol and ethanol mixtures than for the methanol mixture. By fitting the data and extrapolating, the infinite diameter detonation velocities can be estimated for the solutions; these were 7010, 6680, and 6400 m/s for the solutions with glycerol, ethanol, and methanol, respectively. The reaction zone lengths were also estimated to be on the order of 20-30 mm, which led the authors to conclude that the peroxide mixtures had sensitivities just lower than nitroglycerine. The report also describes measurements in which two detonation velocities are apparent, with the lower velocities near 2000-3000 m/s. Low velocity detonation can be associated with liquid explosives, due to the incomplete release of available chemical energy, but typically occur with low initiation inputs or external experimental difficulties with the confinement.<sup>8</sup> This has been observed in mixture explosives, in which only one constituent reacts leaving the others unreacted. Also, in the case of liquid explosives, if the sound velocity of the confining material is too high compared to that of the liquid explosive, the shock waves in the confinement travel faster than those in the liquid, resulting in 2-D wave interactions that can produce cavitation ahead of the front, and other complex interactions.

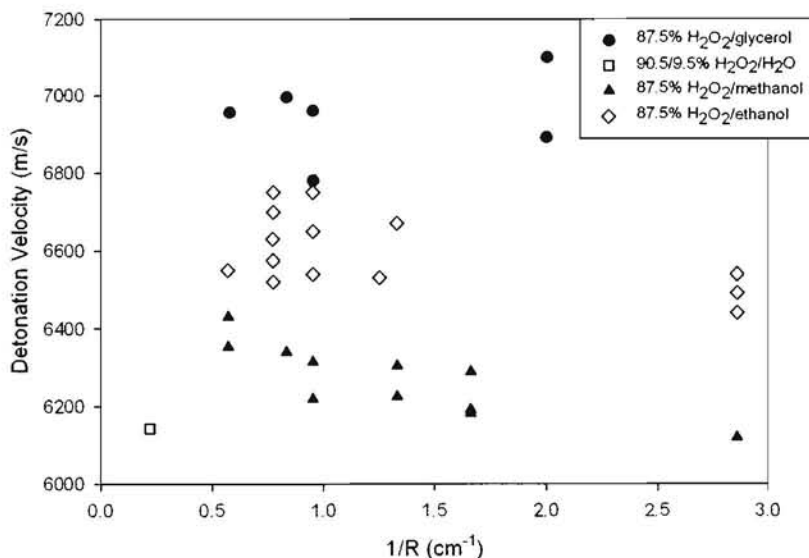


**Figure 1.** Diameter effect curves for H<sub>2</sub>O<sub>2</sub> mixtures from Ref. 2 and the LANL measurement of ~90/10 wt% H<sub>2</sub>O<sub>2</sub>/H<sub>2</sub>O given in Ref. 1.

More recently, Proud and Field<sup>9</sup> employed spectroscopic tools under shock compression to detect UV/Visible emissions from ~ 99.6 wt% hydrogen peroxide/water solutions. The authors assert that the material underwent shock-induced chemical reaction at 70 °C under a stimulus of the drive from a detonator ( $P \sim 5$  GPa, shock pulse duration of 2  $\mu$ s).

Our own study was undertaken to verify estimates of the Hugoniot and detonation properties of a range of H<sub>2</sub>O<sub>2</sub>/H<sub>2</sub>O mixtures presented in Ref. 1 in which sound velocity measurements, Cheetah calculations, and a single good measurement of detonation velocity of a 90/10 H<sub>2</sub>O<sub>2</sub>/H<sub>2</sub>O mixture were performed and used to make the estimates.

**Table 1.** Calculated CJ velocities and pressures, and von Neumann spike conditions for several concentrations of H<sub>2</sub>O<sub>2</sub>/H<sub>2</sub>O solutions (see Ref. 1)

Wt % H <sub>2</sub> O <sub>2</sub>	Calc $D_{CJ}$ <sup>a</sup> (mm/ $\mu$ s)	Corrected $D_{CJ}$ <sup>b</sup> (mm/ $\mu$ s)	Est spike $P$ <sup>c</sup> (GPa)	Calc $P_{CJ}$ <sup>a</sup> (GPa)	Corrected $P_{CJ}$ <sup>d</sup> (GPa)
85.0	5.50	6.06	19.0	7.9	9.5
90.0	5.73	6.27	21.0	8.9	10.6
90.5	5.75	6.29	21.2	9.0	10.7
92.5	5.83	6.37	22.0	9.4	11.2
95.0	5.93	6.48	23.2	9.9	11.8
97.5	6.03	6.58	24.4	10.4	12.4
100.0	6.12	6.68	25.5	10.9	13.0

<sup>a</sup>Calculated using CHEETAH code. <sup>b</sup>Corrected using measured detonation velocity. <sup>c</sup>Estimated using corrected  $D_{CJ}$  and the unreacted Hugoniot. <sup>d</sup>Corrected using a constant gamma relationship explained in Ref. 1.

The critical diameter of 90.5/9.5 wt% H<sub>2</sub>O<sub>2</sub>/H<sub>2</sub>O solution was determined to be  $43.2 \pm 2.2$  mm at 29.0 °C.<sup>1</sup> The temperature corrected detonation velocity of this solution was estimated to be 6.294 km/s.<sup>1</sup> By combining the experimental results, insights from CHEETAH calculations, and the Hugoniot predictions, the detonation values given in Table 1 were estimated.

Here, we present new measurements on high concentration peroxide solutions that provide corroborating data and new information to that presented in Ref. 1.

## EXPERIMENTAL PROCEDURE

### DETERMINATION OF H<sub>2</sub>O<sub>2</sub> CONCENTRATIONS

Highly concentrated H<sub>2</sub>O<sub>2</sub> was obtained from FMC, and stored in glass containers. The concentration of H<sub>2</sub>O<sub>2</sub>/H<sub>2</sub>O solutions was determined according to literature methods by measurement of the refractive index using a refractometer, see below.<sup>10-11</sup> The solutions studied here were ~98 and 95 wt% H<sub>2</sub>O<sub>2</sub>.

The refractive index data of Ref. 11 have been extrapolated to other temperatures in order to provide % H<sub>2</sub>O<sub>2</sub> vs. refractive index vs. temperature plots to make it relatively easy to determine the concentration if the refractive index and temperature are known. Figure 2 shows these plots; a) for concentrations from 90 to 100 wt% H<sub>2</sub>O<sub>2</sub>/H<sub>2</sub>O solutions and b) for concentrations from 80 to 90 wt% H<sub>2</sub>O<sub>2</sub>/H<sub>2</sub>O.

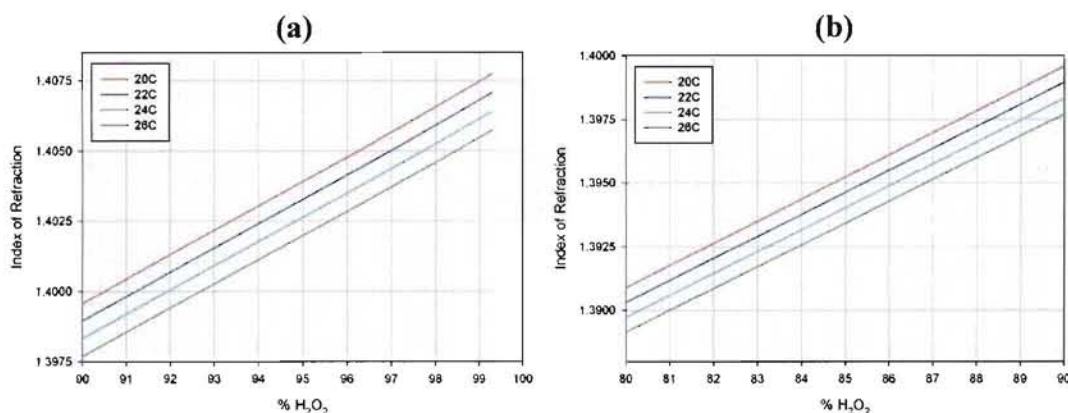


**Figure 2.** Plots of index of refraction vs. H<sub>2</sub>O<sub>2</sub> concentration for several temperatures. Data from Ref. 11 have been extrapolated to other temperatures.

### GAS GUN-DRIVEN PLATE IMPACT EXPERIMENTS

A significant challenge to studying the shock-induced reactions and initiation characteristics of concentrated peroxide solutions is their time-sensitive reactivity with surrounding confining materials. In particular, we are interested in understanding the initiation characteristics of hydrogen peroxide (H<sub>2</sub>O<sub>2</sub>) solutions that react, in an oxidative fashion, with many organic materials used in typical gas gun target sample cells, including most epoxies. To surmount this obstacle, a Remote Liquid Loading System (RLLS), described previously,<sup>12</sup> has been designed, implemented, and evaluated on the LANL large-bore (50 mm) two-stage light gas gun.<sup>13</sup> The system was designed to allow for loading of high-hazard liquid materials into instrumented target cells immediately prior to gas gun firing and is described below.

In the experiments, H<sub>2</sub>O<sub>2</sub> solutions were contained in a polymethylmethacrylate (PMMA) target cells as shown in Fig. 3. The top and bottom angled pieces of the cell were made of PMMA (PMMA is compatible with high concentration H<sub>2</sub>O<sub>2</sub> for periods of up to a day based on compatibility tests performed in-house). The gauge membrane (60 μm thick) was a glued-together sandwich of two pieces of 25 μm FEP Teflon with 5 μm thick Al (etched to produce a gauge pattern) between the sheets. The gauge package was glued on the 30° angle of the target cell bottom; and then the top piece was glued to it. A single element gauge (stirrup gauge) was glued to the Kel-F 81 top (carefully made flat and parallel) and then it was glued and screwed to the cell using nylon screws.

A schematic of the cell (which can contain ~25 mL liquid volume) is shown with fill holes on the side in Fig. 3. Our initial experiments, which were not remotely loaded, were configured in

this way. When it was decided to remotely load the cells, the fill holes were made in the back of the cell with 1/8 inch pipe tap holes so that the fill lines could be attached to the cell as shown in Fig. 4. The cells were remotely loaded from the bottom up as will be indicated later.

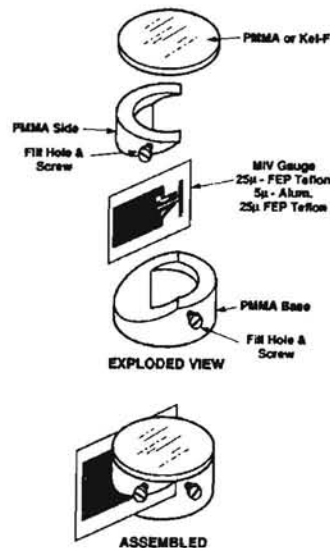


**Figure 3.** Cell used to contain the highly concentrated  $H_2O_2$  solutions – both an exploded view and the assembled unit.

All experiments were conducted on a gas-driven two-stage gun with a launch tube bore of 50 mm and a maximum projectile velocity capability of  $\sim 3.5$  km/s. It was necessary to use the high velocities achievable with this gun because of the insensitivity of the high concentration  $H_2O_2$ , as with related liquid explosives. The projectile velocity was measured to an accuracy of  $\sim 0.1\%$  using an optical interrupt system located at the end of the barrel. Gas gun projectiles were made of Lexan with Kel-F 81 impactors in the front. The gas gun has an electromagnet mounted in the target chamber that produces a uniform 1200 Gauss field in gauge region. The electromagnetic gauge membrane had nine particle velocity and three “shock tracker” gauges. The stirrup gauge, in contact with the liquid, provided an additional measurement at the liquid input interface. The magnetic gauge method used in this study is discussed in Ref. 13.

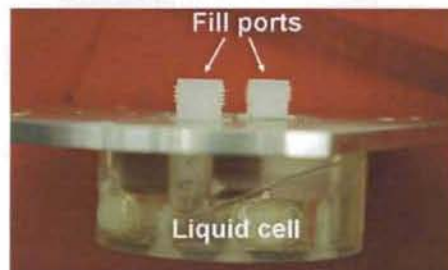


**Figure 4.** Side view of liquid target cell showing the fill ports on the back of the target. Also visible is the side of the gauge membrane which has been glued into the cell on a  $30^\circ$  angle with the cell front. The cell front is at the bottom of the picture.

#### GAS GUN REMOTE LIQUID LOADING SYSTEM

A Remote Liquid Loading System (RLLS) has been designed, implemented, and evaluated on the LANL large-bore (50 mm) two-stage light gas gun.<sup>12</sup> A photograph of the RLLS implemented at the gun facility is shown in Fig. 5. The system was designed to allow for loading of high hazard liquid materials into instrumented magnetic gauge target cells immediately prior to gas gun firing. The system was tested using high concentration ( $\sim 98$  wt%)  $H_2O_2/H_2O$  solutions. The details of the RLLS are presented in Ref. 12. The loading of the liquid, using a gravity feed,

filled the cell from the bottom with almost no bubbles in ~150 seconds, and the experiment was shot ~180 seconds after loading began. Two video cameras mounted on the back of the target were aimed at the target cell to allow observation of target loading to ensure an absence of bubbles in the cell. Bubbles are known to be highly sensitizing because they form localized regions of high temperature and pressure (or "hot spots") resulting from hydrodynamic collapse of the bubbles under shock compression.



**Figure 5.** RLLS is shown as implemented on the LANL two-stage gas gun. The H<sub>2</sub>O<sub>2</sub> reservoir and several valves are located on a plate situated so that the components are above the target cell inside the target chamber to facilitate a gravity feed to the cell. There is also a large container of water on the plate that allows flushing the system after an experiment.

The RLLS was tested before and during the experiments which are described below. Parameters, such as flow rate, were adjusted after each experiment to get the filling operation to go smoothly and minimize the problems with bubbles forming due to turbulence.

## RESULTS AND DISCUSSION

### GAS GUN EXPERIMENTAL RESULTS

Several experiments were done prior to installing the remote loading system with no success. The H<sub>2</sub>O<sub>2</sub> chemically reacted with the glue bonds over time and produced bubbles. There were also problems with the glue bonds breaking and other related problems. In the early experiments, the cells were loaded up to 3 hours before they were shot because of the procedures associated with firing the two-stage gas gun. The failure of the early experiments drove the decision to develop a remote loading system that would minimize many of these problems with the goal of firing the shot two to three minutes after loading of the peroxide solution into the target cell.

Seven gas gun experiments have been completed to date using the remote loading system. The results have been mixed because we were troubleshooting the procedure, including

fine-tuning of the flow rate and making modifications to the valve system in order to control the peroxide loading to minimize the bubbles formed during the loading process. The experimental data has gotten better as a function of time because of the fine tuning.

### H<sub>2</sub>O<sub>2</sub>/H<sub>2</sub>O SOLUTION UNREACTED HUGONIOT

Ultrasonic measurements of the sound velocity of several concentrations of hydrogen peroxide solutions were reported in Ref. 1 and it was found that, in general, the sound speeds as a function of hydrogen peroxide concentration were well-represented by the function:

$$c_0 = (A + Dx^B)/(1 + x^B) \quad (1)$$

where  $x = [\text{wt\% H}_2\text{O}]/C$ , and  $A = 1.488 \pm 0.004 \text{ mm}/\mu\text{s}$ ,  $B = 1.636 \pm 0.183$ ,  $C = 105.8 \pm 29.5$ , and  $D = 2.090 \pm 0.153 \text{ mm}/\mu\text{s}$ .<sup>1</sup> By knowing the bulk sound velocity, the unreacted Hugoniot (equation of state) of the H<sub>2</sub>O<sub>2</sub>/H<sub>2</sub>O solutions can be estimated using a relationship known as the Universal Liquid Hugoniot(ULH)<sup>4</sup>:

$$U_s = c_0[1.37 - 0.37 \exp(-2u_p / c_0)] + 1.62u_p \quad (2)$$

where  $c_0$  is the bulk sound velocity at ambient conditions. This relationship has been found to hold for numerous liquids in the regime of unreacted behavior (e.g. moderate shock pressures). The relationship allows the Hugoniot behavior of numerous concentrations to be estimated rapidly, and further compared to Hugoniot data derived from the plate impact experiments below.

Six experiments have provided unreacted Hugoniot data for the ~98 wt% mixtures. The Hugoniot loci were determined by analysis of the response of the embedded electromagnetic gauges. The input particle velocity is derived from the response of the stirrup gauge at the PMMA/solution interface, and the shock velocity is determined *on non-reactive experiments* from the arrival time of the shock at the known Lagrangian positions of the "shock tracker" elements, as well as the nine individual particle velocity gauge elements. In the experiments where there was reaction, some unreacted shock velocity data can be obtained from the early gauge signals and early shock tracker signals. Hugoniot data from the experiments are tabulated in Table 4. Some of these values are subject to change as the data are scrutinized more carefully as a function of time.

In some cases, the stirrup gauge data were not as good as one would have hoped for (noisy, etc.), for reasons that are not yet well understood, but may have to do with material features. Because of this, there is more scatter in the Hugoniot data than would be normally expected in our plate-impact experiments. In the case of 2s-376, there was no available shock velocity data because the experiment detonated rapidly so the unreacted Hugoniot point was obtained by impedance matching, using the projectile velocity and the Kel-F 81 Hugoniot. The same is true for shot 2s-428. In the case of 2s-395, there was a lot of scatter in the data, both the stirrup gauge and the shock velocity from various sources, so this point is felt to have larger error than the others and will not be included in the plot. The data are plotted in shock velocity in Fig. 6. From the shock velocity ( $U_s$ ) and particle velocity ( $u_p$ ) estimated using the ULH, the Rankine-Hugoniot conservation relations can be used to determine other descriptors of the shocked states (pressure, volume, density, energy).

Also plotted in Figure 6 are the unreacted Hugoniots for 100 wt %, 95 wt%, 90 wt%, 85 wt %, and 80 wt % H<sub>2</sub>O<sub>2</sub> mixtures based on the estimates from the bulk sound speed and ULH. They are all very close together and the data points fall on or near the predictions. This means the estimates made in Ref. 1 are valid, and provide accurate estimates of the mixture Hugoniots. It also indicates that measurements of the unreacted Hugoniots aimed at distinguishing between the Hugoniots for various mixtures in this range would be very difficult to make.

**Table 4.** Hugoniot data derived from H<sub>2</sub>O<sub>2</sub>/H<sub>2</sub>O solution plate impact experiments.

Shot No.	H <sub>2</sub> O <sub>2</sub> wt%	Proj. Vel. km/s	Particle Velocity, mm/μs	Shock Velocity, mm/μs	Pressure, GPa	Comments
2s-368	97.7	2.921	1.57	4.83	10.8	No reaction
2s-376	97.4	3.417	1.91	5.50	15.0	Heterogeneous Init. Detonation
2s-377	98.2	3.273	1.82	5.2	13.5	Homogeneous Init. Detonation (some problems)
2s-394	98.5	3.272	1.81	5.2	13.3	Homogeneous Init. Detonation (almost perfect)
2s-395	95.2	3.137	1.70	5.4	13	No reaction (late time perturbations)
2s-428	97.2	3.350	1.84	5.4	14.5	Homogeneous Init. Detonation (good wave profiles)
2s-431	96.8	3.061	1.68	5.04	12.1	No reaction

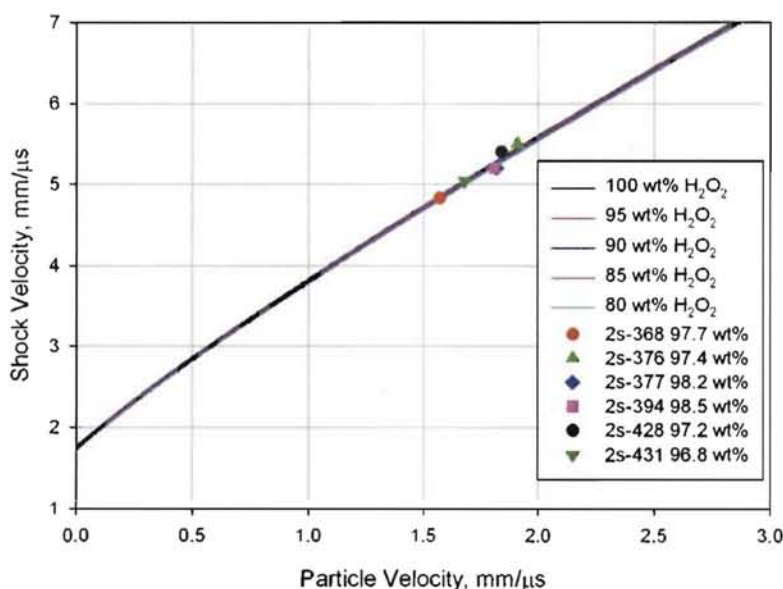


**Figure 6.** Hugoniot data for ~98 wt% H<sub>2</sub>O<sub>2</sub>/H<sub>2</sub>O solutions overlaid with the predicted Hugoniots for 80-100 wt% H<sub>2</sub>O<sub>2</sub>/H<sub>2</sub>O from the ULH relation.

### SHOCK INITIATION MECHANISM

The initiation mechanism of liquid explosives is thought to be derived from thermal explosion at a plane near the shock input interface, behind the initial shock which produces a reactive wave that grows and overtakes the initial shock.<sup>14-16</sup> In plate impact experiments, a shock wave is imparted to a liquid explosive sample from the flyer plate impact at a front target plate interface. The incident shock compresses and heats the liquid, resulting in a thermal explosion near the impact interface, and behind the shock front. This is fundamentally different than the mechanism for heterogeneous explosives, in which reactive growth occurs from the

coalescence of hot spots, and subsequent energy release close to the shock front. This makes the shock wave grow at the front, often with reaction behind the front also.

The use of embedded electromagnetic gauges allows for in-situ measurements of the shock and detonation wave profiles, and offers unprecedented insight into the initiation characteristics of the explosives. Figure 7 shows example shock wave profiles from the initiation of NM.<sup>17</sup> In this example, the initial shock has a particle velocity of  $\sim 1.75$  km/s. The wave profile at the impact interface (black) shows a nominally flat top shock in the NM. At a later time/distance into the sample, a reactive wave grows from thermal explosion near the front. This reactive wave grows until (as is the case in the experiment shown in Fig. 7) it reaches a steady condition or overtakes the front. This steady wave is often referred to as a “superdetonation” as the wave travels at velocities considerably exceeding the steady detonation velocity of the explosive because it is propagating into a pre-compressed material. Finally, the reactive wave or superdetonation overtakes the initial shock resulting in an overdriven detonation (at approximately 1.4  $\mu$ s in the Fig. 7), which settles down to a steady detonation with distance.

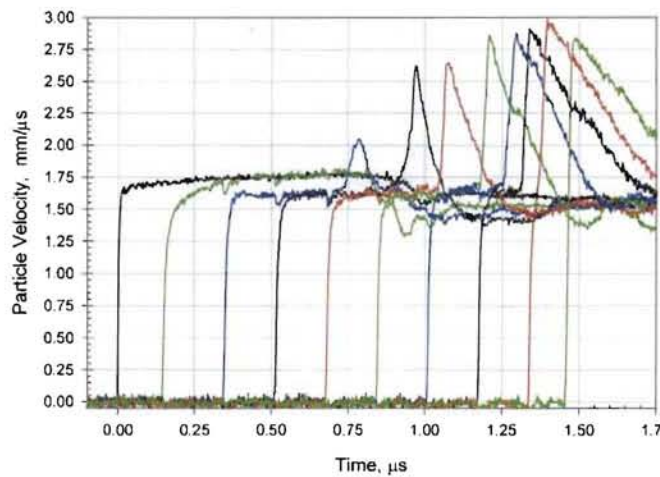


**Figure 7.** Example wave profiles from the shock-to-detonation transition in neat NM solution. This homogeneous reaction mechanism is discussed in Ref. 17.

This mechanism is further elucidated in the t-x diagram in Fig. 8<sup>14</sup>, which is a modification of that proposed by Campbell, Davis and Travis, and Chaiken.<sup>16,15</sup> The figure shows the initial shock traveling into the material, with thermal explosion occurring at some time following initial shock compression not too far from the input interface. A reactive wave resulting from the thermal explosion then builds up over measurable time and distance until it overtakes the initial shock. In the case shown in the figure, it forms a superdetonation before it overtakes the original shock.

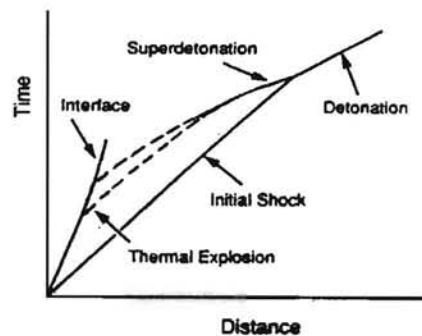


**Figure 8.** T-x diagram describing the homogeneous shock initiation mechanism of liquid explosives.<sup>14,17</sup>

This mechanism has been shown to hold for NM, NM:DETA mixtures, isopropyl nitrate, and other liquid explosives. Based on the wave profiles for Shots 2s-394 and 2s-428 shown in Fig. 9, it is clear that highly concentrated hydrogen peroxide *without bubbles* initiates by this mechanism as well, although it appears that a superdetonation is not achieved before overtake occurs. This homogeneous initiation model may be universal for all homogeneous liquid explosives, since the above examples represent very different types of explosives with very different chemical makeups, detonation energies, and products. The hydrogen peroxide solutions used in this study are chemically the most different of all the other liquid explosives and they still initiate by this mechanism.

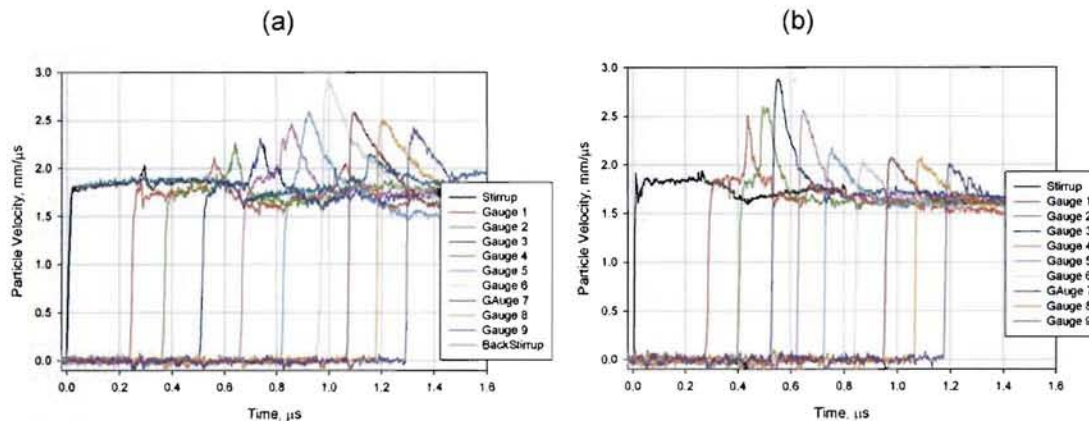


**Figure 9.** Particle velocity waveforms obtained from experiments 2s-394 in (a) and 2s-428 in (b). The homogeneous initiation model described above clearly is the initiation process in these two experiments, with the initial shock, building reactive wave, overtake with overdrive, and then settling down to a steady detonation.

#### SHOCK INITIATION SENSITIVITY (POP-PLOT)

A Pop-plot for liquid explosives is a log-log graph of input pressure vs. time-to-overtake of the initial shock by the reactive wave behind it. The preliminary Pop-plot data for four experiments, Fig. 10, indicate that the highly concentrated (~ 98%)  $H_2O_2/H_2O$  solution *without bubbles*, is less sensitive than neat NM, and much less sensitive than NM:DETA mixtures; e.g. the pressure needed to initiate 98 wt %  $H_2O_2/H_2O$  > neat NM > 95:5 NM:DETA. If one looks at an overtake time of 1  $\mu s$ , the pressures are 13.5 GPa for 98 wt%  $H_2O_2/H_2O$  > 9.5 GPa for neat NM > 7 GPa for 95/5 wt% NM/DETA. Incidentally, 95 wt % NM: 5 wt% DETA (known as Piccatiny Liquid Explosive or PLX) is measurably more sensitive than neat NM or the highly concentrated hydrogen peroxide studied here. Likewise, the addition of "grit," such as 6 wt % rough silica particles shown in Fig. 10, is also sensitizing, as the initiation mechanism changes to a heterogeneous initiation mechanism, i.e., one driven by hot spots that are formed from shock wave interactions with the dispersed particles. The hydrogen peroxide point on the right with the arrow pointing to the right is from experiment 2s-431 where there was no reaction observed but there most likely would have been reaction if the experiment could have been thicker and had a longer time to start. The red line, roughly drawn to indicate the relationship, is only an estimate and will need to be supplemented with additional data to clearly establish it. Notice that the NM data also has some scatter in it.

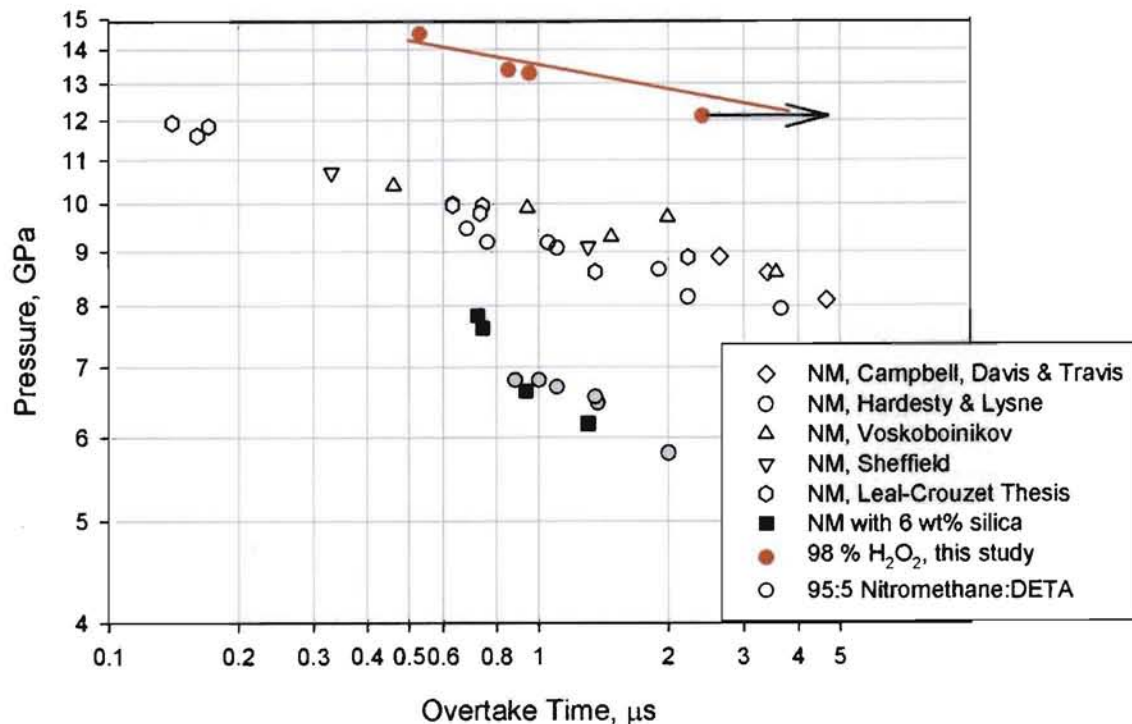


**Figure 10.** Preliminary Pop-plot for 97.5 wt% H<sub>2</sub>O<sub>2</sub>/H<sub>2</sub>O from shots 2s-377, 2s-394, and 2s-428, compared with literature data for neat NM, NM with 6 wt% silica particles, and 95:5 NM:DETA (PLX). The right-most H<sub>2</sub>O<sub>2</sub> point is from 2s-431 showing that the overtake time would be longer than the 2.4 μs of the experiment.

Further work is needed to complete the Pop-plot for the higher concentrations and determine how the shock sensitivity changes with decreasing peroxide concentration to the limits of initiability. Furthermore, additional studies examining the sensitization/desensitization relationships of peroxide solutions with added organic materials should be pursued.

### DETONATION VELOCITY

While the experiments performed here using the embedded gauges only record the shock/detonation wave profiles over approximately 1 cm into the sample, some measurements of the detonation wave velocities have been made with the shock trackers. Follow up experiments, performed in the same way by gas gun-driven plate impact but over longer charge lengths for probing of steady detonation characteristics, will be pursued at a later date.

In two of the experiments, shots 2s-394 and 2s-428, we have been able to measure what appear to be steady detonation velocities of 6.65 km/s. These can be compared to what was estimated in Ref. 1. This has been done in Fig. 11 where Fig. 5 of Ref. 1 is reproduced with these points on it. The two triangles are the data from this work and come from the center tracker. They are a little higher than the line which may be because they are infinite diameter (1-D) measurements where the other measurement is in a stainless steel tube not too much larger than the critical diameter. If these H<sub>2</sub>O<sub>2</sub>/H<sub>2</sub>O mixtures are like other liquid explosives, the velocity deficit (the difference between infinite diameter detonation velocity and detonation velocity near failure) may be small and this is why they are near the line (6.65 km/s vs. 6.6 km/s on the line).

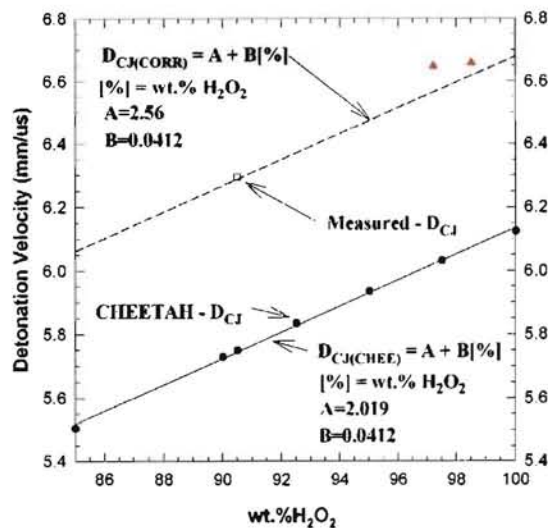


**Figure 11.** Reproduction of Figure 5 from Ref. 1 with the detonation velocities from shots 2s-394 and 2s-428 plotted as red triangles.

## SUMMARY AND CONCLUSIONS

We have presented the results of our early efforts to gain insights into the shock initiation behaviors of highly concentrated hydrogen peroxide solutions. The highly reactive nature of the solutions with their surrounding required the implementation of a remote-loading apparatus for the LANL large bore two-stage gas gun, which was proofed with ~98 wt% H<sub>2</sub>O<sub>2</sub> solutions. The data have been used to determine that the estimates made for the unreacted Hugoniot using the ULH in Ref. 1 are very good estimates for ~98 % hydrogen peroxide solutions. Initiation experiments have yielded Pop-plot information which indicates that ~98% hydrogen peroxide is less sensitive than other liquid explosives, such as NM or PLX, *when not sensitized by entrained bubbles*. Detonation velocities measured as the detonation was becoming steady were measured to be 6.65 mm/ $\mu$ s, slightly above those predicted in Ref. 1. This was expected since they represent infinite diameter (1-D) detonation velocities because of the design of the experiments. In addition, we found that the solutions studied initiated by the same mechanism as other homogeneous liquid explosives – e.g. via thermal explosion and formation of a reactive wave behind the initial shock, which strengthens and overtakes the original shock, forming an overdriven detonation that settles down to a steady detonation.

## FUTURE WORK

Additional work is needed to fully define the Pop-plot for this class of materials, including mapping out the shock initiation behaviors for lower concentration solutions, down to the limits of shock initiability. Insights into the spike and CJ conditions from measurements of the reaction zone would also support the development of reactive burn models for hydrogen peroxide solutions. Future work could also include examining mixtures of hydrogen peroxide/water solutions with organic materials.

## ACKNOWLEDGMENTS

The authors gratefully acknowledge funding from DOE/NNSA Campaign. Los Alamos National Laboratory is operated by Los Alamos National Security, LLC, for the United States Department of Energy under contract DE-AC52-06NA25396.

## REFERENCES

1. Engelke, R., Sheffield, S. A., Davis, L. L., **Experimental and Predicted Detonation Parameters for Liquid-Phase H<sub>2</sub>O<sub>2</sub>/H<sub>2</sub>O Mixtures**, *J. Phys. Chem. A.*, **104**, 6894 (2000).
2. **"Concentrated Hydrogen Peroxide. Summary of Research Data on Safety Limitations,"** Shell Chemical Company report, 1961.
3. Schreck, A. et al., *J. Hazard. Mat.* **A108**, 1 (2004).
4. Woolfolk, R.W. et al. *Thermochimica Acta*, **1973**, 5, 409.
5. Campbell, G. A.; Rutledge, P. V. *J. Chem. E. Symp. Ser.* **37**, No. 33 (1972).
6. Haeuseler, E. *Explosivstoffe* NR 6/7, 64 (1953).
7. Bureau of Mines Staff, U.S. Bureau of Mines Inform. Circ. No 8387, 1968.
8. Engelke, R.; Sheffield, S. A. **"Initiation and Propagation of Detonation in High Explosives,"** in *High Pressure Shock Compression of Solids III*, L. Davidson and M. Shahinpoor, Eds, Springer, 1998.
9. Proud, W. G.; Field, J. E.; *Shock Compression of Condensed Matter-1999*, 937 (2000).
10. Giguere, P. A., *Can. J. Res.* **21**, 156 (1943).
11. McPherson, M. D. "Comparison of densitometry, refractive index, and classical permanganate titration assay methods with commercially available rocket-grade hydrogen peroxide," *Proc. 2<sup>nd</sup> Int. Conference on Green Propellants for Space Propulsion*, Cagliari, Sardinia, Italy, **557**, 67 (2004).
12. Gibson, L. L. et al. *Shock Compression of Condensed Matter-2009*, accepted for publication.
13. Sheffield, S. A., Gustavsen, R. L., Alcon, R. R., **In-situ magnetic gauging technique used at LANL – method and shock information obtained**, AIP Conference Proceedings 505 part 2, p. 1043-1048, 1999.
14. Sheffield, S.A., Engelke, R., Alcon, R.R., **In-situ study of the chemically driven flow fields in initiating homogeneous and heterogeneous nitromethane explosives**, *Proc. 9<sup>th</sup> Sym. (Int'l) on Det.*, Office of Naval Research Report OCNR 113291-7, p. 39, 1989.
15. Chaiken, R. F. *J. Chem. Phys.*, **33**, 760 (1960).
16. Campbell, A. W., Davis, W. C., Travis, J. R., *Phys. Fluids* **4**, 498 (1961)
17. Sheffield, S. A., Engelke, R., **Chapter 1, Condensed Phase Explosives: Shock Initiation and Detonation Phenomena**, in *Shock Wave Science and Technology Reference Library*, Volume 3, Y. Horie (Ed), Springer-Verlag Berlin Heidelberg, 2009.